

**International Journal of Nuclear Energy Science and Technology**

ISSN online: 1741-637X - ISSN print: 1741-6361

<https://www.inderscience.com/ijnest>

---

**Real-time sub-assembly identification through IMU data fusion with vision sensor for an inspection system**

A. Thirumalaesh, N.A. Nibarkavi, S. Joseph Winston, Joel Jose, P.D. Rathika

**DOI:** [10.1504/IJNEST.2023.10058231](https://doi.org/10.1504/IJNEST.2023.10058231)

**Article History:**

Received:	27 August 2021
Last revised:	05 April 2022
Accepted:	08 April 2022
Published online:	07 August 2023

---

## Real-time sub-assembly identification through IMU data fusion with vision sensor for an inspection system

---

### A. Thirumalaesh\*

Robotics and Automation Engineering,  
PSG College of Technology,  
Coimbatore, Tamil Nadu, India  
Email: thirumalaeshraj@gmail.com

\*Corresponding author

### N.A. Nibarkavi

Robotics and Automation Engineering,  
PSG College of Technology,  
Coimbatore, Tamil Nadu, India  
Email: nanibarkavi5@gmail.com

### S. Joseph Winston

Remote Handling and Irradiation Experiments Division,  
Indira Gandhi Centre for Atomic Research,  
Kalpakkam, Tamil Nadu, India  
Email: winston@igcar.gov.in

### Joel Jose

Steam Generator Inspection Devices Section,  
Indira Gandhi Centre for Atomic Research,  
Kalpakkam, Tamil Nadu, India  
Email: joel@igcar.gov.in

### P.D. Rathika

Robotics and Automation Engineering,  
PSG College of Technology,  
Coimbatore, Tamil Nadu, India  
Email: pdr.rae@psgtech.ac.in

**Abstract:** The Prototype Fast Breeder Reactor (PFBR) is a two loop, sodium cooled, pool type reactor. The PFBR reactor core is made up of sub-assemblies holding core material in a hexagonal lattice. The Reactor Core Viewing System in Room Temperature (RCVS-RT) aids in the process of inspection of the reactor core components. It introduces a vision probe into the extracted sub-assembly slot to reach the grid plate top for inspection. This work explores

fusing non-contact sensors to a vision sensor to achieve orientation recognition of the RCVS-RT since the orientation is completely lost during the deployment of camera probe. We achieve this by overlaying generated orientation information from non-contact sensors onto the vision data. We use the orientation of the RCVS-RT and the core geometry to generate a numbering scheme of the adjacent sub-assemblies. This allows for a straightforward identification of the subassemblies in the core while maintaining sterility of core components.

**Keywords:** PFBR; RCVSRT; data fusion; orientation identification; sub-assembly numbering algorithm.

**Reference** to this paper should be made as follows: Thirumalaesh, A., Nibarkavi, N.A., Winston, S.J., Jose, J. and Rathika, P.D. (2023) 'Real-time sub-assembly identification through IMU data fusion with vision sensor for an inspection system', *Int. J. Nuclear Energy Science and Technology*, Vol. 16, No. 2, pp.80–96.

**Biographical notes:** A. Thirumalaesh is currently a Masters student in Robotics at the University of Michigan – Ann Arbor. His areas of research include on state estimation, SLAM and multi-agent localisation. He holds student research positions at the Hybrid Dynamics and Machines Laboratory, Biologically Inspired Robotics and Dynamical Systems Laboratory and Ford Center for Autonomous Vehicles at the University. He completed his Bachelors in Robotics and Automation from PSG College of Technology and holds experience in industrial automation and mobile robotics. His hobbies include experimenting with deep learning, exploring various social sciences and listening to music.

N.A. Nibarkavi is currently pursuing her Masters in Robotics at the University of Michigan – Ann Arbor. She is a research student at the University of Michigan Field Robotics Group. Her current research is on underwater robotics focusing on shipwreck detection, multi-sensor fusion and 3D reconstruction of underwater environments. She was employed as a R&D engineer at Hachidori Robotics, Bangalore where she developed algorithms for autonomous mobile robot navigation and mobile guided vehicles for industrial material movement. She did her Bachelors in Robotics and Automation from PSG College of Technology her hobbies include playing racquet sports.

S. Joseph Winston completed MTech in Machine Design and is working as Head Remote Handling & Irradiation Experiments Division at Indira Gandhi Centre. His area of specialisation is vision based calibration of robotic systems using rigid body parameters. His area of work is robot kinematics, dynamics and control. His interest lies in developing intelligent algorithms for robot controls. He is currently pursuing PhD in the area of vision based rigid body estimation for industrial inspection robot calibration at Indian Institute of Technology, Madras (IITM). He has photography as hobby and writes poems and a lot of python code snippets during leisure time.

Joel Jose completed his BTech in Electronics and Communication and joined Department of Atomic Energy in 2009. He is from the 53rd Batch of BARC Training School. He completed his MTech in 2013 from Homi Bhabha National Institute. He has specialised in the area of robotics and automation. He worked in the control system development for motion control applications using various embedded platforms and FPGAs. He has specialisation in the distributed control for serial and mobile robotic applications using fieldbus protocol CAN. He also worked on the process control application using PLC and HMI. His hobby is reading which he does in his leisure time.

P.D. Rathika is working as Assistant Professor in the department of Robotics and Automation Engineering, PSG College of Technology, India since 2019. She began her career with Cognizant Technologies and has transformed into a teaching enthusiast and researcher. Her research interests include Computer Vision, Image Processing, Information Security and Machine Learning. She has obtained her doctorate in the domain of Convolutional Neural Networks for solving issues in computer networks.

---

## 1 Introduction

The reactor core of Prototype Fast Breeder Reactor undergoes inspections during the commissioning stage. The use of Reactor Core Viewing System in real time serves the purpose. The Reactor Core Viewing System in Room Temperature (RCVS-RT) consists of two sideward angled cameras to view the neighbouring sub-assembly and one camera for straight view. By rotating the camera tube, a complete 360° viewing is achieved. The control panel has a display and a DVR to store the camera feed for processing. The RCVS-RT is capable of horizontal, vertical and rotational motions. When using the rotational motion, once the RCVS-RT is extended into an extracted sub-assembly of the core, information on the orientations of the camera is completely lost. It is always required to ascertain the sub-assemblies in view to identify and also to report on the inspected parameters. The paper proposes a multiple sensor data fusion-based approach where the data from the sensors are combined through a sensor fusion algorithm which gives out contextual meaning to individual sensor data (Hall and Llinas, 1997). The use of an IMU sensor to extract information on orientation of the cameras, which when fused with the output of the vision sensor advocates for information that simplifies the job of the operator.

## 2 Data fusion

Data fusion techniques combine multiple sensor data and related information to obtain improved accuracies and detailed inferences than could be achieved by the use of a single sensor alone (Hall and Llinas, 1997). Using data fusion in multi-sensor environments is primarily done to obtain a lower error probability and a higher reliability by using data from multiple distributed sources (Castanedo, 2013).

Based on the relations of the sources given by Durant-Whyte (1988), our application is classified as complementary type since the information provided by the input sources (camera, GY87) represents different parts of the scene (video, orientation) which is used to obtain a holistic global information. We obtain the identity of the visible sub-assembly by way of its logical numbering followed to identify each individual sub-assembly.

Dasarathy's (1997) data fusion classification indicates this system as data in-feature out (DAI-FEO) since the data fusion process employs raw data (orientation) from the sources to extract features (deviation from north) that describe an entity in the environment.

Abstraction level classification proposed by Luo et al (2002), indicates that this system combines signal level and symbols since the signals are directly acquired from the sensors and the feature is represented as a symbol based on which further decisions are

made. Here, multiple level information fusion occurs since data are provided from different levels of abstraction.

In this work a centralised architecture (Castanedo, 2013) is used, where the fusion node resides in the central processor that receives the information from all of the input sources. In this schema, the sources obtain only the observation as measurements and transmit them to a central processor, where the data fusion process is performed.

The process of communication between the sensors and the Raspberry Pi module is achieved through Inter Integrated Circuit (I2C). I2C (Mankar et al., 2014) is a serial communication protocol, so data is transferred bit by bit along a single wire (SDA line). The sampling of bits is synchronised by a clock signal shared between the master (Raspberry Pi) and the slave (GY87) making it synchronous. The clock signal is controlled by the master always. It can support n number of masters and an upper limit of 1008 slaves. I2C uses only two wires (SCL-Serial Clock, SDA-Serial Data). In this project, I2C is selected as the mode of communication for its simple wiring and its availability on the chosen hardware.

### 3 Prototype fast breeder reactor

#### 3.1 Prototype fast breeder reactor-- design

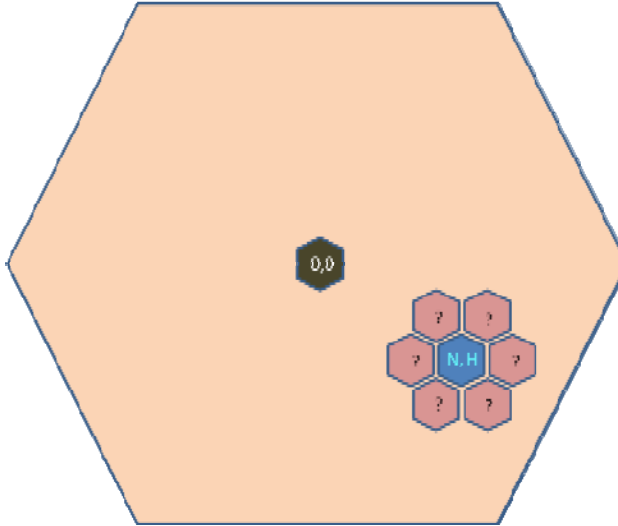
PFBR in India is a 500 MWe power and sodium cooled pool type reactor which utilises the  $\text{UO}_2\text{-PuO}_2$  fuel. The reactor has the state of art technologies with concepts such as grid plate, primary pipes, fuel handling system, top shield (Chellapandi et al., 2011). The primary sodium circuit is contained in a large diameter vessel named the main vessel and contains core, primary pumps, intermediate heat exchanger, primary pipe connecting the pumps and the grid plate. The vessel has no penetrations and is welded to the roof slab on the top. The main vessel uses cold sodium for cooling that enhances its structural integrity. The core sub-assemblies are supported on the grid plate, which in turn is supported on the core support structure. The main vessel is surrounded by the safety vessel, with a nominal gap of 300 mm that allows robotic and ultrasonic inspection of the vessels.

#### 3.2 Reactor core

The reactor core has sub-assemblies in hexagonal lattice structure (Raghupathy et al., 2004). Each hexagonal structure that is a sub-assembly is surrounded by six other sub-assemblies except at the extremities. During the inspection, the camera is used to ascertain the core structural integrity and foreign entities if any, to be identified and removed by the RCVS-RT. The physical deformities can be analysed through image processing to obtain quantifications for the same. The numbering scheme for each of the hexagon is in the form of  $[n, h]$ . 'n' is the sub-assembly row ID, while 'h' is named the sub-assembly number in each respective row. If the hexagons are visualised as being imprinted on the circumferences of concentric circles, n represents the row number, h represents the position of the hexagon in the nth row. The values of n range in  $[0, x]$ . x represents the number rows of sub-assembly present in the core. The values of h ranges between  $[1, 6n]$  for the hexagons in any given row of the numbering 'n'. At any given time, when a sub-assembly is extracted and the RCVS-RT is deployed, the numbering of

the neighbouring sub-assemblies can be computed analysing the numbering pattern. The numbering to be identified is represented in the Figure 1.

**Figure 1** Sub-assemblies notation scheme



## 4 Hardware

The Raspberry Pi acts as a centralised controller to control motion of linear actuator and data acquisition for Vision and IMU sensors. This set up is to be mounted on the RCVS-RT. The communication between the IMU sensor and the Raspberry Pi is established using I2C mode of communication. Using I2C allows for a synchronous form of serial communication, that has eliminated wiring complexity. The IMU sensor GY-87 supports I2C connectivity. The MPU6050 accelerometer-gyroscope module along with the HMC5883L magnetometer module was used to extract orientation information. The sensor gives 10 Degrees of Freedom (DOF) information which can be accessed by reading the individual registers of the modules on the integrated circuit. The programming is done in Python using modules including the ‘smbus’ to access the I2C bus. Figure 2 shows the block diagram of the proposed system.

### 4.1 Reactor core viewing system – real time

During the pre-commissioning stage, the RCVS would be used to perform inspection before sodium is filled in the main vessel. Thus, RCVS is operated at Room Temperature (RT) conditions. There is a requirement for this Reactor Core Viewing System (RCVS) in order to visually examine reactor core components focusing on viewing the neighbourhood of the fuel sub-assembly array through the extracted sub-assembly whose dimensions are shown in Figure 3.

Figure 2 Block diagram of the system

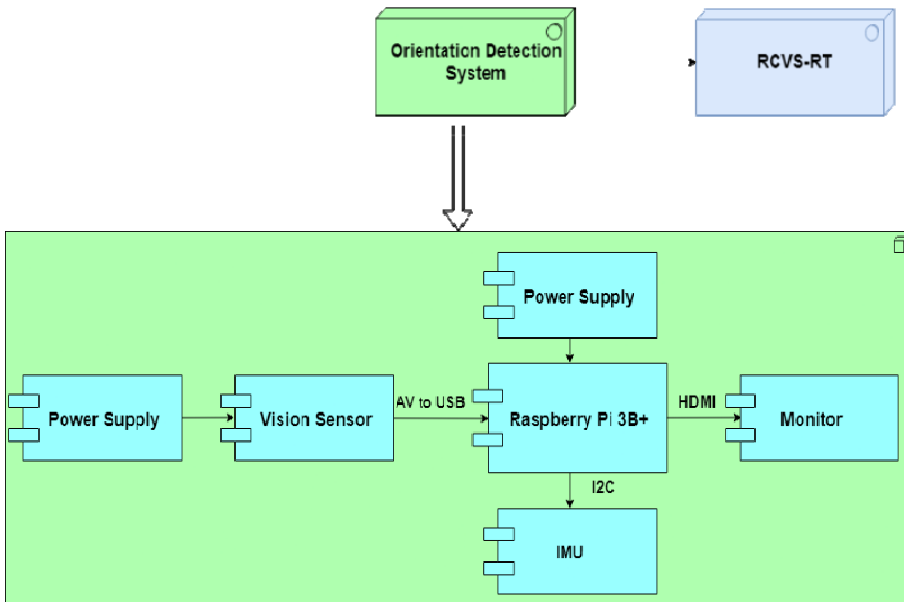
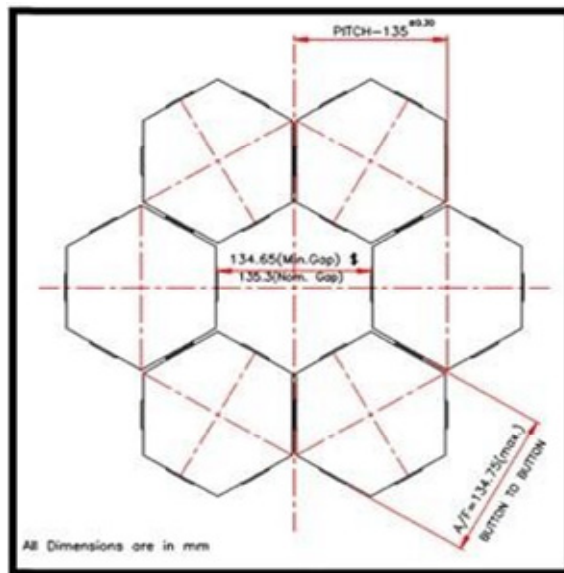
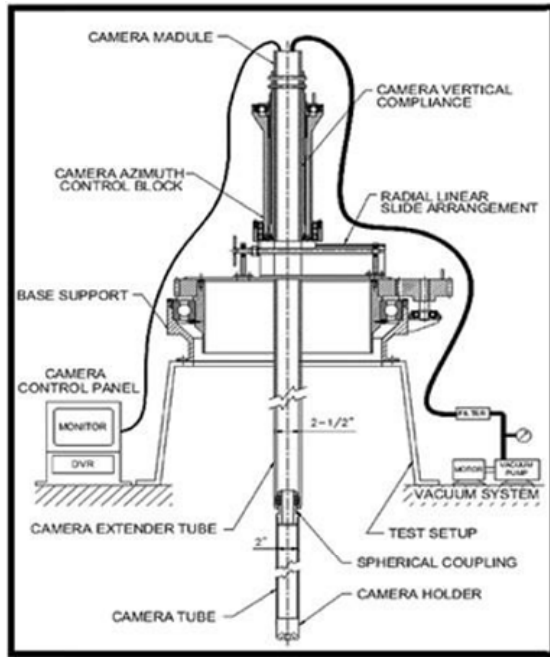


Figure 3 Cross-section of sub-assembly



The RCVS is a remote viewing inspection tool mounted on the flange of the observation port on the roof slab of the reactor. It will enter into the core through the slot of extracted sub-assembly to gain viewing access of the grid plate. The general layout of the system is as shown in Figure 4.

**Figure 4** Layout of reactor core viewing system



Pipes and tubes of the camera pass through the radial linear slide sub-module. It has linear and radial axes which enables the correct positioning of the RCVS. It helps position the long structure of RCVS and thus locates the visual unit above the vacant sub-assembly on top the grid plate. The ranges of motion of lead screw and pinion is shown in Table 1 which is used to change the camera angle.

**Table 1** Actuators motion parameters

<i>Motion</i>	<i>Actuation</i>	<i>Range</i>	<i>Resolution</i>
<i>R</i>	Lead screw	200 mm	0.5 mm
<i>θ</i>	Pinion	360°	3.3°

GY-87 is a 10 Degree of Freedom sensor module consisting of six-axis MPU6050, a three-axis magnetometer HMC5883L and a digital barometer BMP180. It is advantageous with the presence in-built low noise linear low-dropout voltage regulator, on board filters for noise and high current and in-built logic level converter for I2C communication protocol.

In MPU6050, a three-axis gyroscope and a three-axis accelerometer is embedded on the same silicon board with onboard Digital Motion Processor that can handle complex Motion Fusion algorithms.

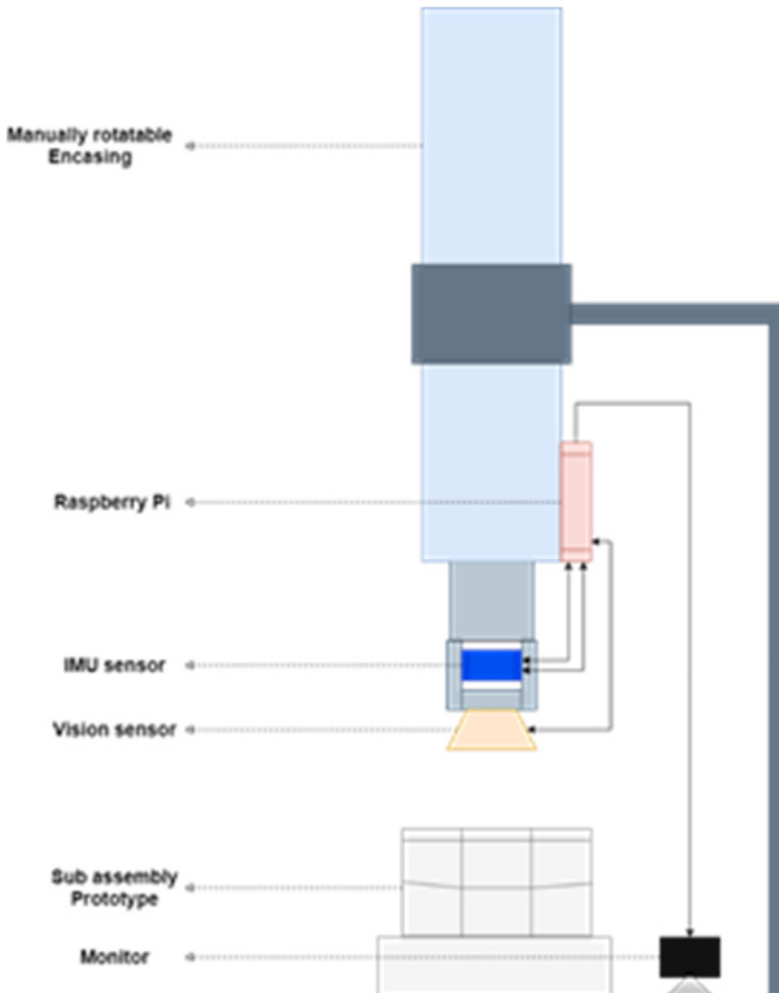
The HMC5883L is a surface mount multi-chip module designed for low field magnetic sensing with a digital interface for applications of low-cost compassing and magnetometry. In this application, using HMC588L it is possible to extract the North bearing angle information and use it to track the deviation from the same.



All these are available in a small sized ( $2.2\text{cm} \times 1.7\text{cm}$ ) chip weighing 6g. The low-cost chip combined with its size and accuracy which led to its selection. The accelerometer and gyroscope can be used to account for motions for application involving angular motions in three axes. Using MPU6050, the roll, pitch and yaw values are also computed to account for any tilt.

In Figure 5, the experimental setup schematic that contains the camera, IMU sensor and other components is shown.

**Figure 5** Schematic of the experimental setup

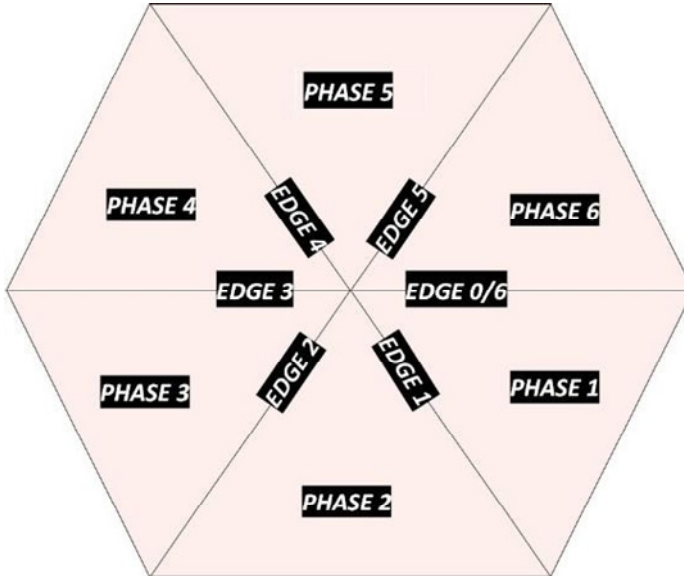


## 4.2 Algorithm

The algorithm developed is based on identified patterns of the numbering scheme of the hexagonal lattice. Patterns identified are classified as phase, edge and exceptions as shown in Figure 6. The identified pattern is used to produce the list of possible

surrounding subassemblies. The list is then correlated to the sensor data i.e., North angle information, to pick the numbering of the current sub-assembly that the RCVS is oriented towards.

**Figure 6** Classification of the identified patterns



The system takes input from the IMU sensor and the vision sensor. Using data fusion, the output of a video feed display with a compass and numbering of the seen sub-assembly is shown. Primarily, it makes use of the values of ( $N$  and  $H$ ) entered to determine the sub-assembly row ID of the extracted sub-assembly. With a range of 1 to 6 for the phase number, it is determined by choosing the first value ‘ $x$ ’ which satisfies (1)

$$\frac{H}{N * 6} \leq \frac{x}{6}$$

Using the phase number, the numbering algorithm can be applied. The use of python programming and its modules, allows for a simplistic implementation of the algorithm. Reduced complexity in interfacing the sensor and the camera to the Raspberry Pi, modules to access the I2C bus, usage of the NumPy module to simplify shifting operations are the advantages of using Python as the programming language.

Then, OpenCV module is used to perform image augmentation operations. A dynamic line is superimposed on the video feed that traces the North throughout the inspection process. Another line that points the sub-assembly faced is also superimposed. Then, current [ $n$ ,  $h$ ] values are also displayed on the screen. This gives the user intuition to guiding the RCVS-RT in the directions required.

### 4.3 Numbering algorithm

The aim is to identify six pairs of  $[n, h]$  that corresponds to the numbering of the six neighbouring sub-assemblies. In order to do so, the plane is divided into six phases. Discernible patterns are identified in the six phases for  $n$  and  $h$ .

The six numbering patterns can further be generalised, since a cyclic rotation of the pattern of any phase ‘ $p-1$ ’, leads to the pattern of the phase ‘ $p$ ’. However, these patterns break down along the edges of each of the phases, wherein the numbering pattern is shared between the individual patterns of the two intersecting phases. The convention of the numbering scheme is shown in Figure 7. The various cases are detailed below.

*Case 1:* For the given lattice, when a clockwise numbering of 1 to 6 starting from the vertical axis is used to number each phase, the list of the values of ‘ $n$ ’ for neighbouring sub-assemblies of any sub-assembly in phase 1 is given by:

$$N_p = [n, n+1, n+1, n, n-1, n-1] \tag{2}$$

The sequence for the values of ‘ $h$ ’ of neighbouring sub-assemblies for the same is given by:

$$H_p = [h-1, h+(phase\_no-1), h+phase\_no, h+1, h-(phase\_no-1), h-phase\_no] \tag{3}$$

The positions of  $[n, h]$  as described in (2) and (3) is shown in Figure 8.

**Figure 7** Numbering schemes of the sub-assembly

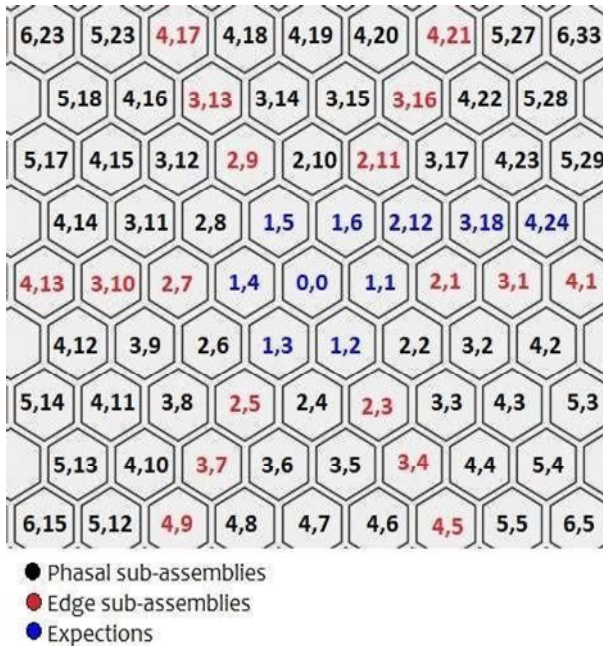
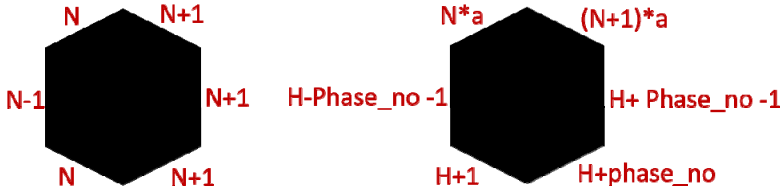


**Figure 8** General pattern for phase sub-assemblies



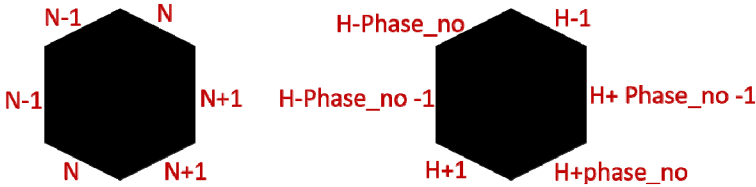
These sequences when they undergo a right shift, produce the sequence of the values for phase 2 and so on.

*Case 2:* When the extracted sub-assembly lies in between two phases, the sequences follow a pattern unlike the above. For such edge conditions, the list of  $[n, h]$  for neighbouring sub-assemblies of the extracted sub-assembly residing between phases 1 and 6 is given by:

$$\begin{aligned}
 Ne &= [n+1, n+1, n+1, n, n-1, n] \\
 n+1*a, h(\text{phase\_no}-1), h+\text{phase\_no}, h+1 \\
 h-(\text{phase\_no}-1), n*a
 \end{aligned} \tag{4}$$

where ‘a’ is the edge number ranging between 0 and 5. The positions described in (4) and (5) is illustrated in Figure 9.

**Figure 9** General pattern for edge sub-assemblies

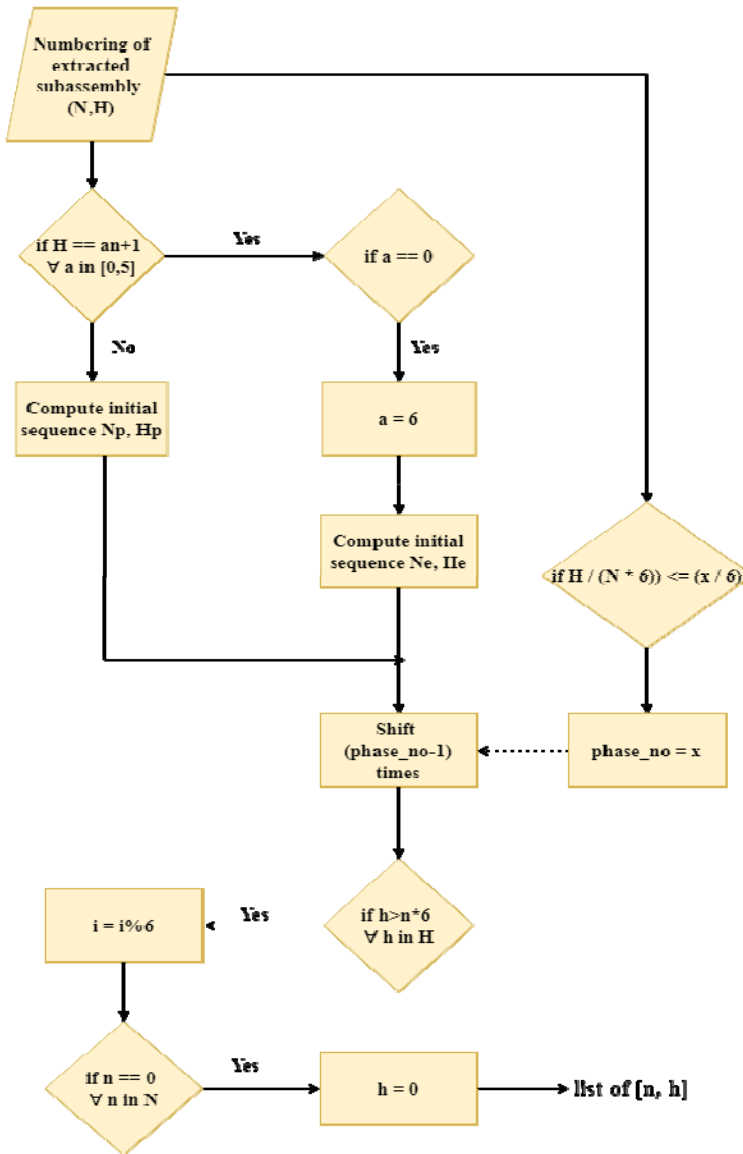


These sequences when they undergo a right shift, produce the sequence of the values for neighbours of sub-assemblies between phases 1 and 2 and so on.

*Case 3:* There are exceptions to the developed numbering algorithm. One such occurs when the extracted sub-assembly has the configuration of  $H=6N$ . It is identified when any  $h$  exceeds  $6n$  and thus  $h$  is reassigned using the remainder operator. Another exception is for if  $n$  equals 0,  $h$  is also set to 0. For when the extracted sub-assembly is the centre i.e.,  $N=0, H=0$ , the numbering algorithm is void, and thus surrounding sub-assemblies are output directly based on angular data.

The following flowchart, depicts the algorithm used for finding the neighbouring sub-assembly details. As shown in Figure 10, the input of  $N$  and  $H$  is used to compute the output list of six  $[n, h]$  pairs. Initially, the extracted sub-assembly is verified for its position in a phase or edge. Following which, a general list is computed. This is later then shifted based on the location of the extracted sub-assembly. The output is a list of six neighbouring  $[n, h]$  pairs in the clockwise order, starting from the vertical axis.

Figure 10 Flowchart of numbering algorithm



## 5 Experiment and results

Initial implementation involved connecting the Raspberry Pi over Wi-Fi to a VNC Viewer for testing algorithm functioning and code debugging. Here, for validation of results, a mobile phone's compass was used as reference. The developed algorithm was then tested on a 1:1 prototype of the sub-assembly setup. The system hardware including Raspberry Pi, Vision and IMU sensor was mounted on a mechanical structure

representing the RCVS as shown in Figure 11. It is essential to mount the GY87 in the same gradient as the central camera to get accurate reading about North bearing angle. The metal structure holds a manually rotatable and vertically movable pipe that emulates the motions of the RCVS. A close view is available in Figure 12.

**Figure 11** Experimental setup



**Figure 12** Top view of experimental setup



Vision camera was given regulated power supply. The Raspberry Pi was powered separately while sensor received power via Raspberry Pi. In the 1:1 prototype, the central sub-assembly has been left open which can be interpreted as any extracted sub-assembly. The six surrounding hexagonal structures are the surrounding sub-assemblies whose indices are to be identified.

The sensor was ensured to be along the same planar inclination as the camera. A monitor was connected via Raspberry Pi HDMI. The output seen during trials are shown below for multiple cases. In the following images, the red line represents the North, that is being tracked by the IMU sensor, while the blue line stands as the reference that points the sub-assembly to which the RCVS is oriented towards. The  $[n, h]$  on the top left corner shows the numbering algorithm output to which the blue line also points towards.

Figure 13 shows the location of the extracted sub-assembly (Chellapandi et al., 2011; Dasarathy, 1997) in the core and a schematic representation of the test result. Figure 14, shows the result obtained for when the extracted sub-assembly is off phase 1.

**Figure 13** Schematic of [7, 4] location and test result

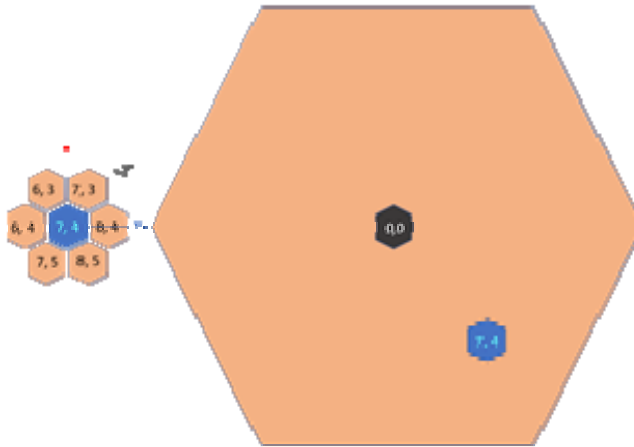


**Figure 14** Output for sub-assembly [7, 4] in phase 1

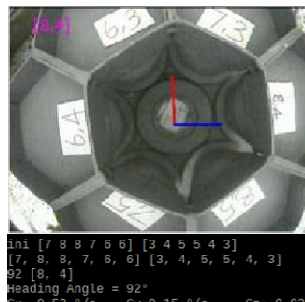


Figure 15 shows the location of the extracted sub-assembly [6, 13] (Raghupathy et al., 2004) in the core and a schematic representation of the test result. Figure 16, shows the result obtained for when the extracted sub-assembly is off edge 2.

**Figure 15** Schematic of [6, 13] location and test result

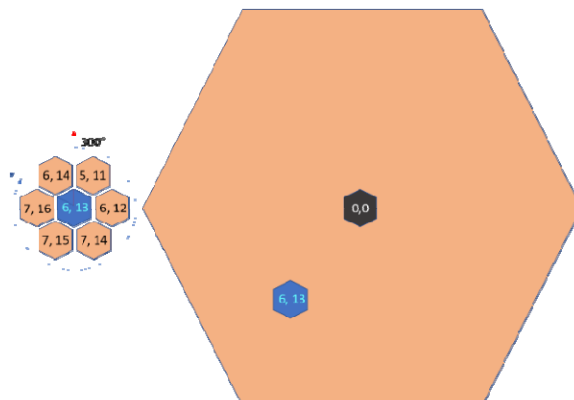


Figure 16 Flowchart of numbering algorithm

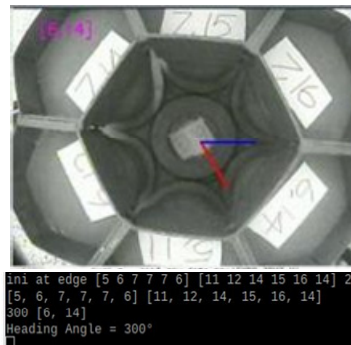


Figure 17 shows the location of the extracted sub-assembly [4, 24] (Dasarathy, 1997) in the core and a schematic representation of the test result. Figure 18, shows the result of an exceptional case. This exception is for when  $H$  is  $6N$ .

Figure 17 Schematic of [4, 24] location and test result

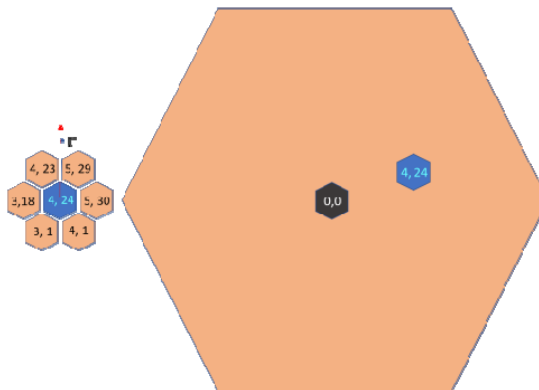


Figure 18 Output for sub-assembly [4, 24] in phase 6

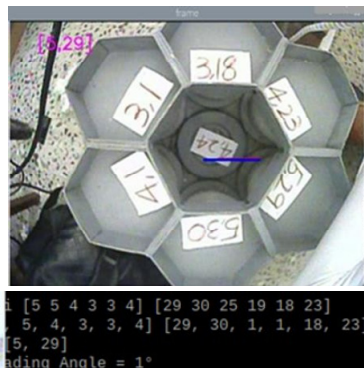
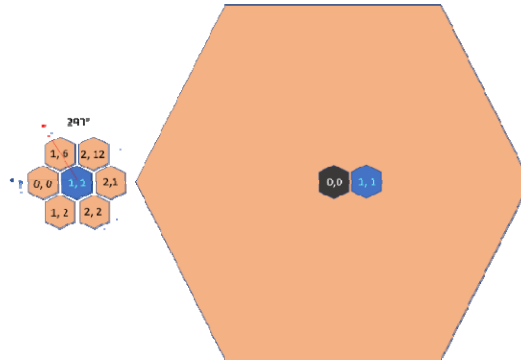


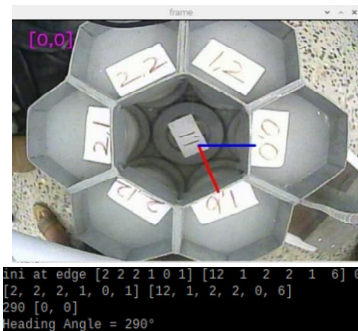


Figure 19, shows the location of the extracted sub-assembly (Hall and Llinas, 1997) in the core and a schematic representation of the test result. Figure 20, shows the result of another exceptional case. This is for considering  $h=0$  when  $n=0$ .

**Figure 19** Schematic of [1, 1] location and test result



**Figure 20** Output for [1, 1] in edge 6



## 6 Conclusion

The real-time sub-assembly identification system is designed for the orientation identification of the Reactor Core Viewing System. The system has been tested with 1:1 mock test setup and provides dynamic numbering of the neighbouring sub-assemblies with respect to selected sub-assembly. With this sub-assembly indication, the operator can easily carry out visual inspection of the core. The complete use of the IMU sensor can also aid in the future prospects of improving the system. The accelerometer and the gyroscope on the MPU6050 can be used to obtain supplemental safety information on the deformation of the RCVS, if any. Any deformation, especially tilts can be identified using the IMU. Also, the development of a complete software module that can include other image processing techniques such as quantising properties of any structural deformities is possible. The use of I2C in this project limits the distance of data lines that can be used and thereby reinforces placing controller nearby. This can be overcome by

studying the usage of RS485 or any serial bus that can transmit over long distances which allows data acquisition from a remote location. Initial calibration of the sensor would be necessary at time of deployment and periodic checks would be necessary. Also, sensor positioning has to be done precisely, and offsets from centre if any, will have to be accounted for.

## References

- Castanedo, F. (2013) 'A review of data fusion techniques', in Maxwell, C. (Ed.): *A Treatise on Electricity and Magnetism*, pp.68–73.
- Chellapandi, P., Puthiyavinayagam, P., Balasubramaniyan, V., Raghupathy, S., Babu, V., Chetal, S.C. and Raj, B. (2011) 'Development of innovative reactor assembly components towards commercialization of future FBRs', *Energy Procedia*, Vol. 7, pp.359–366.
- Dasarathy, B.V. (1997) 'Sensor fusion potential exploitation-innovative architectures and illustrative applications', *Proceedings of the IEEE*, Vol. 85, No 1, pp.24–38.
- Durrant-Whyte, H.F. (1988) 'Sensor models and multisensor integration', *International Journal of Robotics Research*, Vol. 7, No. 6, pp.97–113.
- Hall, D.L. and Llinas, J. (1997) 'An introduction to multisensor data fusion', *Proceedings of the IEEE*, Vol. 85, No 1, pp.6–23.
- Luo, R.C., Yih, C.C. and Su, K.L. (2002) 'Multisensor fusion and integration: approaches, applications, and future research directions', *IEEE Sensors Journal*, Vol. 2, No. 2, pp.107–119.
- Mankar, J., Darode, C., Trivedi, K., Kanoje, M., and Shahare, P. (2014) 'Review of I2C protocol', *International Journal of Research in Advent Technology*, Vol. 2, No 1, pp.474–478.
- Raghupathy, S., Singh, O.P., Govindarajan, S., Chetal, S.C. and Bhoje, S.B. (2004) 'Design of 500 MWe prototype fast breeder reactor', *Indira Gandhi Centre for Atomic Research*, pp.1–9.